

See discussions, stats, and author profiles for this publication at: <https://www.researchgate.net/publication/231531042>

# Precision Measurements of Binary and Multicomponent Diffusion Coefficients in Protein Solutions Relevant to Crystal Growth: Lysozyme Chloride in Water and Aqueous NaCl at pH 4.5 an...

ARTICLE in JOURNAL OF THE AMERICAN CHEMICAL SOCIETY · MARCH 1999

Impact Factor: 12.11 · DOI: 10.1021/ja9834834

---

CITATIONS

69

---

READS

76

5 AUTHORS, INCLUDING:



**John Albright**

Texas Christian University

71 PUBLICATIONS 906 CITATIONS

SEE PROFILE



**Onofrio Annunziata**

Texas Christian University

50 PUBLICATIONS 760 CITATIONS

SEE PROFILE



**Luigi Paduano**

University of Naples Federico II

163 PUBLICATIONS 2,315 CITATIONS

SEE PROFILE

# Precision Measurements of Binary and Multicomponent Diffusion Coefficients in Protein Solutions Relevant to Crystal Growth: Lysozyme Chloride in Water and Aqueous NaCl at pH 4.5 and 25 °C<sup>⊥</sup>

John G. Albright,<sup>\*,†</sup> Onofrio Annunziata,<sup>‡</sup> Donald G. Miller,<sup>‡,§</sup> Luigi Paduano,<sup>‡,||</sup> and Arne J. Pearlstein<sup>‡</sup>

Contribution from the Chemistry Department, Texas Christian University, Fort Worth, Texas 76129, Geosciences and Environmental Technologies, Lawrence Livermore National Laboratory, P.O. Box 808, Livermore, California 94551, Department of Mechanical and Industrial Engineering, University of Illinois at Urbana–Champaign, 1206 West Green Street, Urbana, Illinois 61801, and Dipartimento di Chimica, Università di Napoli, Via Mezzocannone 4, 80134 Naples, Italy

Received October 1, 1998

**Abstract:** Accurate models of protein diffusion are important in a number of applications, including liquid–liquid phase separation and growth of protein crystals for X-ray diffraction studies. In concentrated multicomponent protein systems, significant deviations from pseudobinary behavior can be expected. Rayleigh interferometry is used to measure the four elements  $(D_{ij})_v$  of the ternary diffusion coefficient matrix for the extensively investigated protein, hen egg-white lysozyme (component 1) in aqueous NaCl (component 2) at pH 4.5 and 25 °C. These are the first multicomponent diffusion coefficients measured for any protein system at concentrations high enough to be relevant to modeling and prediction of crystal growth or other phase transitions, and the first for a system involving lysozyme at any concentration. The four ternary diffusion coefficients for the system lysozyme chloride/NaCl/water are reported for lysozyme chloride at 0.60 mM (8.6 mg/mL) and NaCl at concentrations of 0.25, 0.50, 0.65, 0.90, and 1.30 M (1.4, 2.8, 3.7, 5.1, and 7.2 wt %), with the latter two compositions being supersaturated. One cross-term,  $(D_{21})_v$ , is 80–259 times larger than the main term  $(D_{11})_v$  and 7–18 times larger than  $(D_{22})_v$ . Standard interferometric diagnostic tests indicate that aggregation is unimportant in our experiments. We also present binary diffusion coefficients  $D_v$  for lysozyme chloride/water at concentrations from 0.43 to 3.08 mM (6.2–44.1 mg/mL), at the same pH and temperature. The precision of the results is about 0.1% for the binary diffusion coefficients and diagonal ternary diffusion coefficients, and about 1–2% for the cross-terms. For the ternary systems investigated, we show that a single pseudobinary diffusion coefficient does not accurately describe diffusive transport, and predictions by simple models such as the Nernst–Hartley equations are inaccurate at the higher concentrations considered here. Finally, dynamic light-scattering diffusion coefficients, differing from both our interferometrically measured  $(D_{ij})_v$  and a theoretical prediction of light-scattering diffusion coefficients in multicomponent systems, are reported for the same solutions used for the ternary experiments at 1.30 M.

## Motivation

Diffusion plays a role in many biochemical processes. In particular, diffusion of proteins is important in a number of in vivo, laboratory, medical, and manufacturing applications. Examples include centrifugation and other separations, dialysis, and crystallization. Effective modeling, prediction, and design of these processes require accurate descriptions of protein transport. Since buffers, added salts, or other macromolecules are typically present, such systems are invariably multicomponent in nature.

The complete description of an  $n$ -solute system requires an  $n \times n$  matrix of diffusion coefficients relating the flux of each

solute component to the gradients of all solute components.<sup>1</sup> Since experience with other multicomponent systems shows that cross-terms  $((D_{ij})_v, i \neq j)$  are often significant, the validity of the common assumption of pseudobinary protein diffusion can be assessed only by measuring the full set of  $n^2$  diffusion coefficients.<sup>1,2</sup>

One of the most important scientific applications in which protein diffusion is critical is the growth of large crystals with low defect densities, the initial step in the determination of protein structure by X-ray crystallography.<sup>3</sup> Despite considerable effort to understand the fundamentals, protein crystal growth is still as much art as it is science.

A large body of experimental and theoretical work clearly points to the central role of diffusion in several protein crystal growth phenomena. First, diffusion (along with attachment and

\* To whom correspondence should be addressed. Phone: (817) 257-6198. Fax: (817) 257-5851. E-mail: albright@gamma.is.tcu.edu.

† Texas Christian University.

§ Lawrence Livermore National Laboratory.

‡ University of Illinois at Urbana–Champaign.

|| Università di Napoli.

⊥ Portions of this paper were presented in a poster at the 7th International Conference on the Crystallization of Biological Macromolecules in Granada, May 3–8, 1998.

(1) Onsager, L. *Ann. N. Y. Acad. Sci.* **1945**, *46*, 241–265.

(2) Gosting, L. J. In *Advances in Protein Chemistry*; Anson, M. L., Bailey, K., Edsall, J. T., Eds.; Academic Press: New York, NY, 1956; Vol. XI, pp 429–554.

(3) Giegé, R.; Drenth, J.; Ducruix, A.; McPherson, A.; Saenger, W. *Prog. Cryst. Growth Charact.* **1995**, *30*, 237–281.

other kinetic processes) determines the concentration profiles within a protein-depleted zone immediately adjacent to the growing crystal.<sup>4–7</sup> Second, diffusion of precipitant and impurities (including protein impurities) is thought to be critical to incorporation or rejection of these species into or from the growing crystal.<sup>7–9</sup> Third, diffusion is important in establishing the concentration gradients responsible for the buoyancy-driven convective flow that can arise in protein crystal growth experiments under normal (e.g., earth) gravity conditions.<sup>6,9</sup> Finally, when protein crystal growth is conducted under microgravity conditions, diffusion is the dominant transport mechanism.<sup>10</sup>

Due to the importance of protein crystal growth, a substantial effort has been made to develop mathematical models capable of predicting crystal quality and growth rate as a function of growth conditions. The more sophisticated of these models (cf. Lin et al.,<sup>8</sup> Savino and Monti<sup>11</sup>) compute concentration distributions and fluxes based on (1) a more-or-less full treatment of flow in the liquid, (2) diffusive and convective mass transfer in the liquid and at the growing interface, (3) association/dissociation equilibria and kinetics in the liquid, and (4) binding and desorption equilibria and kinetics at the liquid/solid interface.

At the growth interface, incorporation of protein and rejection of supporting electrolyte give rise to a zone adjacent to the crystal in which protein is depleted and other components (e.g., the supporting electrolyte) are usually enriched. Thus, diffusion in protein crystal growth inevitably occurs under conditions for which *no* species has a uniform concentration. This immediately raises the issue of multicomponent diffusion and the likelihood that protein diffusion will be enhanced or hindered by gradients of other diffusing species.<sup>2</sup>

The influence of other species on protein diffusion follows from the one-dimensional flux relations,<sup>1</sup>

$$-J_i = \sum_{j=1}^n (D_{ij})_v \partial C_j / \partial x \quad i = 1, \dots, n \quad (1)$$

in which the cross-term diffusion coefficients (off-diagonal elements  $(D_{ij})_v$ ,  $i \neq j$ ) can be positive or negative. For one solute component ( $n = 1$ ),  $(D_{11})_v$  in eq 1 is just the solute binary diffusion coefficient and will be denoted by  $D_v$ , where the subscript  $v$  denotes the volume-fixed frame of reference. In ternary systems ( $n = 2$ ),  $(D_{11})_v$  and  $(D_{22})_v$  are the main-term diffusion coefficients relating the flux of a component to its own concentration gradient, and  $(D_{12})_v$  and  $(D_{21})_v$  are the cross-term diffusion coefficients relating the flux of each component to the gradient of the other. For some systems (cf. Vitagliano et al.,<sup>12</sup> Albright et al.<sup>13</sup>), a cross-term  $(D_{ij})_v$  can have considerably larger magnitude than the main-term  $(D_{ii})_v$ , as our measurements show for the systems described here.

(4) Miyashita, S.; Komatsu, H.; Suzuki, Y.; Nakada, T. *J. Cryst. Growth* **1994**, *141*, 419–424.

(5) Kurihara, K.; Miyashita, S.; Sasaki, G.; Nakada, T.; Suzuki, Y.; Komatsu, H. *J. Cryst. Growth* **1996**, *166*, 904–908.

(6) Rosenberger, F. *J. Cryst. Growth* **1988**, *76*, 618–636.

(7) Vekilov, P. G.; Monaco, L. A.; Thomas, B. R.; Stojanoff, V.; Rosenberger, F. *Acta Crystallogr., Sect. D* **1996**, *52*, 785–798.

(8) Lin, H.; Rosenberger, F.; Alexander, J. I. D.; Nadarajah, A. *J. Cryst. Growth* **1995**, *151*, 153–162.

(9) Grant, M. L.; Saville, D. A. *J. Cryst. Growth* **1991**, *108*, 8–18.

(10) Pusey, M.; Naumann, R. *J. Cryst. Growth* **1986**, *76*, 593–599.

(11) Savino, R.; Monti, R. *J. Cryst. Growth* **1996**, *165*, 308–318.

(12) Vitagliano, V.; Sartorio, R.; Scala, S.; Spaduzzi, D. *J. Solution Chem.* **1978**, *7*, 605–621.

(13) Albright, J. G.; Mathew, R.; Miller, D. G.; Rard, J. A. *J. Phys. Chem.* **1989**, *93*, 2176–2180.

In the experiments reported here, the volume change on mixing and changes in concentrations across the diffusion boundary are small. Consequently, to a good approximation, the measured diffusion coefficients may be considered to be for the volume-fixed reference frame<sup>14</sup> defined by

$$\sum_{i=0}^n J_i \bar{V}_i = 0 \quad (2)$$

where  $\bar{V}_i$  is the partial molar volume of the  $i$ th species, and the subscript 0 denotes the solvent.

Although the importance of multicomponent diffusion has been recognized in the crystal growth community,<sup>6,15</sup> and accounted for semiempirically in modeling growth of lysozyme crystals in aqueous NaCl,<sup>8</sup> no crystal growth model has properly accounted for multicomponent diffusive transport because the necessary data have been unavailable.

While it is sometimes possible to estimate diffusion coefficients in binary and multicomponent systems, these estimates are generally limited to dilute solutions. For example, the binary and multicomponent Nernst–Hartley (N–H) equations are often useful for dilute electrolytes, including proteins. They are based either on limiting ionic conductances (cf. eqs 76–79 of ref 16, or eq 41 of ref 17) or on limiting tracer ionic diffusion coefficients (cf. eq 167 in ref 2, or ref 18). There have also been great strides in ab initio (hydrodynamic) prediction of diffusivities from protein structure data<sup>19–21</sup> by computing Stokes flow around a rigid body having the approximate “hydrodynamic” shape of the given protein molecule. However, this approach is limited to binary systems at infinite dilution with known counterion type and concentration. Unfortunately, as will be seen below, no current estimation procedure works well in the concentrated multicomponent solutions of interest in crystal growth. Therefore, *experimental* multicomponent diffusion coefficients are essential for accurate modeling of protein transport in this important application, especially in view of the very large cross-term coefficient  $(D_{21})_v$  reported here. Moreover, since protein crystal growth may occur at supporting electrolyte concentrations that bring the system well into a region of supersaturation, the concentration dependence of all the diffusion coefficients should be important, including those contributing directly to the protein flux.

## Previous Studies of Protein Diffusion in Multicomponent Systems

Virtually all studies of protein diffusion have been performed in multicomponent systems. However, except for the pioneering studies of Leaist (see below), all have assumed pseudobinary diffusion of protein, although several have addressed the issue of how the pseudobinary protein diffusion coefficient depends on the concentration of protein or other electrolyte components.

Pseudobinary protein diffusion cannot provide a full description of diffusion processes in the multicomponent systems in which measurements are made, or in those for which such data

(14) Hooyman, G. J.; Holtan, H., Jr.; Mazur, P.; de Groot, S. R. *Physica* **1953**, *19*, 1095–1108.

(15) Wilcox, W. R. *J. Cryst. Growth* **1983**, *65*, 133–142.

(16) Miller, D. G. *J. Phys. Chem.* **1967**, *71*, 616–632.

(17) Miller, D. G. *J. Phys. Chem.* **1967**, *71*, 3588–3592.

(18) Leaist, D. G.; Lyons, P. A. *J. Phys. Chem.* **1982**, *86*, 564–571.

(19) Allison, S. A.; Potter, M.; McCammon, J. A. *Biophys. J.* **1997**, *73*, 133–140.

(20) Brune, D.; Kim, S. *Proc. Natl. Acad. Sci. U.S.A.* **1993**, *90*, 3835–3839.

(21) Smith, P. E.; van Gunsteren, W. F. *J. Mol. Biol.* **1994**, *236*, 629–636.

will be applied in modeling studies and design, or for other purposes. Indeed, assuming pseudobinary diffusion for an  $n$ -solute system ( $n > 1$ ), whose full description requires  $n^2$  diffusion coefficients, can actually be misleading. Gosting<sup>2</sup> pointed out more than 40 years ago, in the context of protein transport, that multicomponent diffusion coefficients are essential in such studies. To our knowledge, the only previous reports of multicomponent protein diffusion coefficients are three papers by Leaist and Hao,<sup>22–24</sup> who studied bovine serum albumin (BSA) or sodium BSA in dilute solution with at least one salt at 25 °C.

Leaist's first paper<sup>22</sup> presents data obtained by the diaphragm cell method, in which only  $(D_{21})_v$  was measured at several pH values, to demonstrate how diffusion of charged BSA affects transport of NaCl. Depending on pH, there is a considerable coupled flux or counterflux of NaCl due to the BSA gradient. The second paper<sup>23</sup> reports the use of the Harned restricted diffusion method to measure the four ternary diffusion coefficients for the system  $\text{Na}_m\text{BSA}$  ( $m = 7$  or 18)/NaCl/water at three NaCl concentrations. Additional NaCl drastically slows down diffusion of  $\text{Na}_m\text{BSA}$ . The third paper<sup>24</sup> reports quaternary diffusion coefficients measured by the Taylor dispersion method for systems containing BSA and either phosphate or citrate buffer components. In these cases, diffusion of BSA produces extremely large coupled fluxes of the buffer electrolyte components.

A fourth paper by Leaist<sup>25</sup> shows that the counterions  $\text{Na}^+$  and  $\text{K}^+$  are responsible for the large increase in the BSA diffusion coefficient in binary aqueous solutions of  $\text{Na}_m\text{BSA}$  ( $m = 2, 4, 7, 16$ , or 23) and  $\text{K}_{23}\text{BSA}$  at pH values larger than 5.5, as measured by the Harned method. More  $\text{Na}^+$  counterions (larger  $m$  values) significantly increase the binary diffusion coefficient of  $\text{Na}_m\text{BSA}$ .

In the three ternary and quaternary studies,<sup>22–24</sup> the measured diffusion coefficients were compared to values predicted at infinite dilution by the extended N–H equations<sup>23,24</sup> or an approximation thereto.<sup>22</sup> These equations use the ion species concentration ratios and the limiting ionic mobilities and charges. In all three studies, some of the  $(D_{ij})_v$  values were in fair agreement with theory, but others differed in sign or significantly in magnitude from predicted values over the composition range considered. All three papers note the value of using the N–H theory to estimate diffusion coefficients at low to moderately low concentrations.

Our measurements are made by the well-established, absolute technique of Rayleigh interferometry<sup>26</sup> in free-diffusion experiments, using a high-precision instrument, as well as by the more common light-scattering approach using a commercial instrument. Recognizing the ease with which light-scattering diffusion coefficients have been and can be measured, the present work has the additional purpose of providing a benchmark for validation and refinement of theories of light-scattering diffusion coefficient measurements for proteins in multicomponent systems.<sup>27</sup>

### Choice of Systems

A large body of work deals with hen egg-white lysozyme (HEWL; hereinafter, lysozyme), typically in aqueous solutions

containing NaCl and sometimes additional electrolytes. This work includes nucleation (cf. Georgalis et al.<sup>28</sup> and references therein), liquid–liquid phase separation (cf. Muschol and Rosenberger<sup>29</sup> and references therein), and crystallization (cf. Pusey<sup>30</sup>), where NaCl serves as a precipitant. To a large extent, the ternary lysozyme chloride/sodium chloride/water system has become the dominant “model” system for experimental and theoretical studies of protein crystal growth. Consequently, we have chosen to investigate this system at 25 °C. In what follows, lysozyme chloride is designated as component 1 and sodium chloride as component 2.

This paper presents the first systematic diffusion study from moderate precipitant concentrations into the supersaturated region of this extensively examined system, and thus provides a complete set of diffusion coefficients necessary to model diffusive transport in lysozyme crystallization from aqueous NaCl solutions at one lysozyme concentration.

There are many previous measurements,<sup>31–45</sup> mostly by light scattering, of pseudobinary lysozyme diffusion coefficients in ternary and other multicomponent systems. Although in none of these references does the electrolyte closely match any considered here, comparison suggests that, when significant supporting electrolyte is present, the pseudobinary diffusion coefficients are usually within 10–20% of our  $(D_{11})_v$  diffusion coefficients for the lysozyme component reported below.

All three-component mutual-diffusion experiments reported here were performed by Rayleigh interferometry at pH 4.5 and at a mean lysozyme concentration (average of top and bottom solution concentrations) of 0.60 mM (8.6 mg/mL). Four experiments, with different combinations of protein and NaCl concentration differences, were performed at each of five mean NaCl concentrations (0.25, 0.50, 0.65, 0.90, and 1.30 M, corresponding to 1.4, 2.8, 3.7, 5.1, and 7.2 wt %), for a total of 20 experiments. We note that experiments must be performed with at least two different concentration differences at each combination of mean concentrations in order to measure the four diffusion coefficients of the system.<sup>46–48</sup> Performing four

(28) Georgalis, Y.; Umbach, P.; Soumpasis, D. M.; Saenger, W. *J. Am. Chem. Soc.* **1998**, *120*, 5539–5548.

(29) Muschol, M.; Rosenberger, F. *J. Chem. Phys.* **1997**, *107*, 1953–1962.

(30) Pusey, M. L. *J. Cryst. Growth* **1992**, *122*, 1–7.

(31) Cadman, A. D.; Fleming, R.; Guy, R. H. *Biophys. J.* **1981**, *37*, 569–574.

(32) Mikol, V.; Hirsch, E.; Giegé, R. *J. Mol. Biol.* **1990**, *213*, 187–195.

(33) Nyström, B.; Johnsen, R. M. *Chem. Scr.* **1983**, *22*, 82–84.

(34) Kuehner, D. E.; Heyer, C.; Rämisch, C.; Fornfeldt, U. M.; Blanch, H. W.; Prausnitz, J. M. *Biophys. J.* **1997**, *73*, 3211–3224.

(35) Sophianopoulos, A. J.; Rhodes, C. K.; Holcomb, D. N.; Van Holde, K. E. *J. Biol. Chem.* **1962**, *237*, 1107–1112.

(36) Eberstein, W.; Georgalis, Y.; Saenger, W. *J. Cryst. Growth* **1994**, *143*, 71–78.

(37) Dubin, S. B.; Clark, N. A.; Benedek, G. B. *J. Chem. Phys.* **1971**, *54*, 5158–5164.

(38) Dubin, S. B.; Lunacek, J. H.; Benedek, G. B. *Proc. Natl. Acad. Sci. U.S.A.* **1967**, *57*, 1164–1171.

(39) Colvin, J. R. *Can. J. Chem.* **1952**, *30*, 831–834.

(40) Foord, R.; Jakeman, E.; Oliver, C. J.; Pike, E. R.; Blagrove, R. J.; Wood, E.; Peacocke, A. R. *Nature (London)* **1970**, *227*, 242–245.

(41) Fuh, C. B.; Levin, S.; Giddings, J. C. *Anal. Biochem.* **1993**, *208*, 80–87.

(42) Baranowska, H. M.; Olszewski, K. J. *Biochim. Biophys. Acta* **1996**, *1289*, 312–314.

(43) Muramatsu, N.; Minton, A. P. *Anal. Biochem.* **1988**, *168*, 345–351.

(44) Nesmelova, I. V.; Fedotov, V. D. *Biochim. Biophys. Acta* **1998**, *1383*, 311–316.

(45) Giordano, R.; Salleo, A.; Salleo, S.; Mallamace, F.; Wanderlingh, F. *Opt. Acta* **1980**, *27*, 1465–1472.

(46) Fujita, H.; Gosting, L. J. *J. Am. Chem. Soc.* **1956**, *78*, 1099–1106.

(47) Fujita, H.; Gosting, L. J. *J. Phys. Chem.* **1960**, *64*, 1256–1263.

(22) Leaist, D. G. *J. Phys. Chem.* **1986**, *90*, 6600–6602.

(23) Leaist, D. G. *J. Phys. Chem.* **1989**, *93*, 474–479.

(24) Leaist, D. G.; Hao, L. *J. Chem. Soc., Faraday Trans.* **1993**, *89*, 2775–2782.

(25) Leaist, D. G. *J. Solution Chem.* **1987**, *16*, 805–812.

(26) Tyrell, H. J. V.; Harris, K. R. *Diffusion in Liquids*; Butterworths: London, 1984.

(27) Leaist, D. G.; Hao, L. *J. Phys. Chem.* **1993**, *97*, 7763–7768.



experiments at each mean composition provides additional confidence in the results and allows for an error analysis.

We have also used Rayleigh interferometry to investigate the concentration dependence of the diffusion coefficient of lysozyme chloride in its binary solution with water. Binary diffusion coefficients are reported for pH 4.5 and mean concentrations 0.4345, 0.6000, 0.8914, 1.7828, and 3.0778 mM (6.2, 8.6, 12.7, 25.5, and 44.1 mg/mL).

Additionally, we have measured dynamic light-scattering diffusion coefficients of the ternary system at 1.30 M NaCl.

## Experimental Section

All experimental work was conducted at Texas Christian University.

**Materials.** Hen egg-white lysozyme, recrystallized six times and lyophilized, was purchased from Seikagaku America. This choice of supplier was guided by the work of Rosenberger and co-workers,<sup>29,49,50</sup> which reports detailed analyses of commercial HEWL products. Two batches of HEWL with different Seikagaku lot numbers and impurity analyses were purchased. The first lot, E96301, had 3.79% moisture and 2.28% chlorine by weight. A later lot, E96Y03, had 4.96% moisture and 1.94% chlorine by weight. Atomic absorption studies at this laboratory showed negligible  $\text{Na}^+$  for both lots. No further purification was performed, since the nonprotein species are present in the diffusion experiments and were accounted for (see below) in determining concentrations. As described below, diagnostic data from binary diffusion experiments were consistent with no proteinaceous contamination.

The molecular mass of the lysozyme solute,  $M_1$ , was taken as  $14\,307\text{ g mol}^{-1}$ , and this value<sup>51</sup> was used to calculate all concentrations after correction for the moisture and chloride content. With these corrections, the effective weight of just the protein was 0.9387 and 0.9304 times the measured weight of the as-received material from lots E96301 and E96Y03, respectively. Buoyancy corrections were made with the commonly used tetragonal lysozyme crystal density<sup>52–54</sup> of  $1.305\text{ g cm}^{-3}$ .

Deionized water was distilled and then passed through a four-stage Millipore filter system to provide high-purity water for all the experiments. The molecular mass of water,  $M_0$ , was taken as  $18.015\text{ g cm}^{-3}$ . Mallinckrodt reagent HCl ( $\sim 12\text{ M}$ ) was diluted by half with pure water and distilled at the constant boiling composition. This resulting HCl solution (approximately 6 M) was then diluted to about 0.063 M (pH 1.2) and used to adjust the pH of solutions.

Mallinckrodt AR NaCl was dried by heating at  $450\text{ }^\circ\text{C}$  for 7 h, taking into consideration the work of Rard,<sup>56</sup> and used without further purification. The purity of the NaCl was listed as 99.9% by the supplier. Its molecular mass,  $M_2$ , was taken to be  $58.443\text{ g mol}^{-1}$  and its crystal density<sup>57</sup> as  $2.165\text{ g cm}^{-3}$  for buoyancy corrections.

**Preparation of Solutions.** Lysozyme from four 25-g bottles of Seikagaku lot no. E96301 was used to prepare solutions for binary experiments LC1, LC2, LC3, and LC4 and the ternary series LNC1,

LNC2, LNC3, and LNC4. The densities of stock solutions (see below) prepared from protein samples taken from three bottles of this lot (based on the weight of the as-received protein) were in fair agreement, but the densities of solutions prepared from samples from the fourth bottle were somewhat higher. For top and bottom solution pairs differing only in protein concentration, those prepared from fourth-bottle samples also had correspondingly larger refractive index increments and larger numbers of fringes. We thus believe that material from this fourth bottle was drier, and that differences in dryness among the protein samples are responsible for some scatter in  $\bar{V}_1$  and the refractive index increments  $R_1$  for the four mean compositions associated with this lot (cf. Table 7). However, all four ternary experiments for each mean composition were done using protein from one bottle and are thus internally consistent. The resulting  $(D_{ij})_v$  vary smoothly with NaCl concentration, despite the small differences in densities, etc., among the protein samples from this lot.

Lysozyme from eight 25-g bottles of Seikagaku lot no. E96Y03 was mixed and stored as a single 200-g batch. Protein used to prepare solutions for binary experiment LC5 and the ternary series LNC5 was taken from this batch. The mean density of the solutions of this set of experiments, based on a long extrapolation, was consistent with lower-concentration values from lot E96301.

All solutions were prepared by mass with appropriate buoyancy corrections. All weighings were performed with a Mettler Toledo AT400 electrobalance. Since the as-received lysozyme powder was very hygroscopic, all manipulations in which water absorption might be critical were performed in a dry glovebox. Stock solutions of lysozyme were made by adding as-received protein to a preweighed bottle that had contained drybox air, capping the bottle, and reweighing to get the weight and thus mass of lysozyme. Water was added to dissolve the lysozyme, and the solution was weighed. An accurate density measurement (see below) was made and used to obtain the molarity of the stock solution.

The top and bottom solutions for each diffusion experiment were prepared by transferring stock protein solution to clean flasks and then diluting and adjusting the pH as follows. For binary experiments, the solutions were first diluted to within  $10\text{ cm}^3$  of the final volumes with pure water. From 1 to 3 mL of the dilute HCl was added to adjust the pH to the desired value, any residual solution on the pH electrode was washed back into the solutions, and the dilutions were completed by mass. The densities and final pH values of these solutions were measured and the final concentrations calculated. For ternary experiments, precise masses of NaCl were added to flasks containing previously weighed quantities of lysozyme stock solutions. These solutions were mixed and diluted to within  $10\text{ cm}^3$  of the final volume. The pH was then adjusted, and the solutions were diluted to their final masses.

Although some series LNC4 solutions (0.90 M NaCl) were supersaturated, crystallization was not observed during the diffusion experiments. However, some series LNC5 solutions (1.30 M NaCl) were well inside the supersaturation region. To prevent crystallization in this series, solution flasks were soaked for at least 1 day in alcoholic NaOH prior to use. The diffusion cell and reservoir were soaked overnight in a solution containing LIQUI-NOX cleaner. We note that visible crystals usually formed in unused series LNC5 solutions after 2 days.

**Measurement of pH.** pH measurements were made using a Corning model 130 pH meter with an Orion model 8102 combination ROSS pH electrode. The meter was calibrated with standard pH 7 and pH 4 buffers and checked against a pH 5 standard buffer. It was assumed that the pH values remained valid at the higher NaCl concentrations. After four or five experiments, the electrode was soaked in 5% NaClO for 10 min, following which the internal reference solution was replaced with fresh solution.

**Density Measurements.** All density measurements were made with a Mettler-Paar DMA40 density meter, thermostated with water from a large, well-regulated ( $\pm 0.01\text{ }^\circ\text{C}$ ) water bath. This instrument is interfaced to a computer for time averaging, and with care consistently gives precision of  $\pm 2 \times 10^{-5}\text{ g cm}^{-3}$  or better.

**Free-Diffusion Measurements.** All free-diffusion measurements were made with the high-precision Gosting diffusometer,<sup>48,58,59</sup> operated in its Rayleigh interferometric optical mode. Data from the Rayleigh

(48) Miller, D. G.; Albright, J. G. In *Measurement of the Transport Properties of Fluids: Experimental Thermodynamics*; Wakeham, W. A., Nagashima, A., Sengers, J. V., Eds.; Blackwell Scientific Publications: Oxford, 1991; pp 272–294.

(49) Thomas, B. R.; Vekilov, P. G.; Rosenberger, F. *Acta Crystallogr., Sect. D* **1996**, 52, 776–784.

(50) Rosenberger, F. *J. Cryst. Growth* **1996**, 166, 40–54.

(51) Canfield, R. E. *J. Biol. Chem.* **1963**, 238, 2698–2707.

(52) Palmer, K. J.; Ballantyne, M.; Galvin, J. A. *J. Am. Chem. Soc.* **1948**, 70, 906–908.

(53) Tanford, C. *Physical Chemistry of Macromolecules*; John Wiley & Sons: New York, NY, 1961.

(54) This value differs by about 6% from a more modern value ( $1.2221\text{ g cm}^{-3}$ ) determined by a different technique<sup>55</sup> and is clearly dependent upon the amount of free and bound water in the crystal. For the purposes of buoyancy correction in weighing, the differences are negligible.

(55) Westbrook, E. M. In *Methods in Enzymology*; Wyckoff, H. W., Hirs, C. H. W., Timasheff, S. N., Eds.; Academic Press: New York, NY, 1985; Vol. 114, pp 187–196.

(56) Rard, J. A. *J. Chem. Thermodyn.* **1996**, 28, 83–110.

(57) Weast, R. C. *CRC Handbook of Chemistry and Physics*, 57th ed.; CRC Press: Cleveland, OH, 1975.

interference patterns were collected with a 6000-pixel, 6-cm linear CCD array with  $10\text{-}\mu\text{m} \times 10\text{-}\mu\text{m}$  pixels, mounted vertically on a precision stage. The stage with this vertical array was stepped horizontally through the two-dimensional interference pattern to collect the data necessary to calculate the diffusion coefficients. Horizontal positions were obtained with an optical encoder with  $\pm 0.5\text{ }\mu\text{m}$  accuracy. Data acquisition was controlled with a Dell Dimension XPS P166s computer, which performed the subsequent data reduction.<sup>59,60</sup> For the first four binary experiments, a magnification factor (1.759 42) was measured using a precision ruled quartz scale (Photo Sciences Inc., Torrance, CA) with 100 lines/cm, whose relative positions are accurate to  $0.25\text{ }\mu\text{m}$ . Because of slight readjustment of the diode array position, a second magnification factor (1.761 06) was measured and used for the remaining binary ( $C_1 = 0.60\text{ mM}$ ) and all the ternary experiments reported here.

A 543.5-nm He–Ne Uniphase laser was used as the light source of the diffusimeter. The free-diffusion experiments were performed in a Tiselius cell (C-1235-H11), with an optical path length of 2.5057 cm. The temperature of the bath was regulated at  $25.00\text{ }^\circ\text{C}$  with a model PTC-41 Tronac temperature controller to a precision of  $\pm 0.001\text{ }^\circ\text{C}$ . All experiments were done at ambient pressure. Filling of cells and boundary sharpening were done by standard procedures,<sup>48,61</sup> with a peristaltic pump replacing gravity as the means of drawing solution into the “siphon” tube to sharpen the boundary. All diffusion boundaries were checked for static and dynamic stability<sup>62</sup> and found to be stable. Calculation of ternary diffusion coefficients was done with the program TFIT<sup>59–61,63</sup> by using data from four experiments with different initial concentration increments across the boundary but with the same mean concentrations of lysozyme chloride and NaCl.

The precision of measurement appears to be better than  $\pm 0.1\%$  for the binary diffusion coefficients and for the main-term diffusion coefficients of the ternary diffusion experiments. The ternary cross-term errors are larger (about 1–2%), as reported by Albright and Miller and co-workers for other ternary systems (cf. Albright et al.,<sup>13</sup> Mathew et al.,<sup>64,65</sup> and Miller et al.<sup>61</sup>).

No attempt was made to remove clusters or other protein aggregates (e.g., by filtration or centrifugation), since the Rayleigh interferometric method (unlike dynamic light scattering) is quite insensitive to the presence of small numbers of high-molecular-weight aggregates, which can be expected to diffuse very slowly and hence contribute little to the fringe patterns. Even if aggregates were present, they would be expected to negligibly affect diffusive transport of monomers, which is the dominant diffusion process during crystal growth.

**Dynamic Light-Scattering Diffusion Coefficients.** Dynamic light-scattering diffusion coefficients,  $D_{\text{DLS}}$ , were measured for samples from all solutions of the ternary series LNC5 (1.30 M NaCl mean concentration).

Measurements were made using a Protein Solutions DynaPro-801 TC molecular sizing instrument with a fixed scattering angle of  $90^\circ$ . Solutions were injected through a  $0.02\text{-}\mu\text{m}$  Whatman Anotop 10 filter. This instrument was interfaced with a Dell Dimension XPS 300-MHz computer for numerical reduction of intensity fluctuation data. The monomodal mode in the Protein Solutions Dynamics V4.0 software package was used in the analysis. Each reported  $D_{\text{DLS}}$  was obtained by averaging intermediate values for at least 1 h of data collection, but there was little change in the  $D_{\text{DLS}}$  average value after a few minutes of data collection. Included with the output from data analysis are four basic diagnostics: (1) polydispersity coefficient, (2) baseline, (3) sum of squares (SOS), and (4) count rate. The polydispersity coefficients

**Table 1.** Binary Experimental and Derived Data at  $25\text{ }^\circ\text{C}$  (Series LC)

expt	LC1	LC5	LC2	LC3	LC4
$\bar{C}_1$ (mM)	0.4345	0.6000	0.8914	1.7828	3.0778
$\Delta C_1$ (mM)	0.3220	0.4000	0.3364	0.6728	0.8516
pH bottom	4.42	4.50	4.48	4.52	4.51
pH top	4.51	4.50	4.48	4.46	4.50
$d$ ( $\text{g cm}^{-3}$ ) bottom	0.999 53 <sub>4</sub>	1.000 35 <sub>2</sub>	1.001 49 <sub>4</sub>	1.005 92 <sub>9</sub>	1.011 57 <sub>8</sub>
$d$ ( $\text{g cm}^{-3}$ ) top	0.998 17 <sub>8</sub>	0.998 68 <sub>4</sub>	1.000 08 <sub>1</sub>	1.003 07 <sub>8</sub>	1.008 02 <sub>4</sub>
$\Delta t$ (s)	20	22	10	8	13
$J$ (meas)	41.818	51.112	43.639	87.630	109.379
$\bar{V}_1$ ( $\text{cm}^3\text{ mol}^{-1}$ )	10 184	10 225	10 296	10 497	10 750
$\bar{V}_0$ ( $\text{cm}^3\text{ mol}^{-1}$ )	18.070	18.069	18.067	18.058	18.033
$R_1$ ( $10^5\text{ dm}^3\text{ mol}^{-1}$ )	1.299	1.278	1.297	1.302	1.284
$D_v$ (meas)	0.5591	0.5443	0.5276	0.4839	0.4407
( $10^{-9}\text{ m}^2\text{ s}^{-1}$ )					
$D_v$ (corr)	0.5678	0.5508	0.5316	0.4858	0.4417
( $10^{-9}\text{ m}^2\text{ s}^{-1}$ )					

were small and indicate nearly monodisperse protein. All baseline values were  $1.000 \pm 0.001$ , all SOS values were negligible, and all count rates were within  $\pm 5\%$ , thus meeting the specifications given in the Protein Solutions manual for a good measurement. That the measurements were not corrupted by retention of protein on the filter was established by measuring  $D_{\text{DLS}}$  for solutions passed through two sequential filters. Measurements of  $D_{\text{DLS}}$  agreed with those for single-pass filtration to within 0.3%, which is approximately the measurement error.

## Results

**Binary Diffusion Coefficients at pH 4.5.** Diffusion coefficients were measured for the lysozyme chloride system in the concentration range from 0.4345 to 3.0778 mM (6.2–44.1 mg/mL). Table 1 shows the results of these measurements and includes the mean concentrations and the concentration increment across the boundary  $\Delta C$ ; pH values of the bottom and top solutions; densities of the bottom and top solutions; mean concentration; fringe number  $J$ ; partial molar volumes  $\bar{V}_i$  of the protein and water; refractive index increment  $R \equiv [\partial n/\partial C]$ ; and measured volume-fixed diffusion coefficient  $D_v$ . General discussions of the experimental theory and nomenclature for the binary and ternary cases are presented elsewhere.<sup>48,66–68</sup>

The time offset  $\Delta t$  is also included, which relates the elapsed time  $t$  of a scan measured on the laboratory clock to the apparent formation time of a step-function starting boundary (free-diffusion boundary conditions). For each scan of an experiment, an average diffusion coefficient  $D_{\text{ave}}$  is obtained by averaging the separate diffusion coefficients  $D_j$  calculated from each symmetrical Rayleigh fringe pair  $j$  of that scan in the range  $0.25 < z_j < 1.0$ , where  $z_j = \text{erfinv}\{(J - 2j)/J\}$ , and  $\text{erfinv}$  is the inverse error function. These average values  $D_{\text{ave}}$  from all scans of an experiment were plotted against their corresponding values of  $1/t$  and extrapolated to  $1/t = 0$  to obtain the values of  $D_v$  shown in Table 1. The slope of this straight line is  $D_v\Delta t$ .

A corrected value of each  $D_v$  is also listed in Table 1. This correction is necessary because, as the lysozyme concentration decreases, the HCl added to maintain the pH at 4.5 is an increasingly large fraction of the total electrolyte. It thus becomes a second solute, and the solution becomes increasingly ternary. The HCl correction is made in four steps as follows:

(1) The limiting tracer diffusion coefficient for the lysozyme ion is assumed to be  $0.12 \times 10^{-9}\text{ m}^2\text{ s}^{-1}$ . This value was obtained within two significant figures from our ternary ( $D_{11}$ )<sub>v</sub> diffusion coefficients, for which the dragging effect of the counterion is almost completely eliminated by the high salt

(58) Gosting, L. J.; Kim, H.; Loewenstein, M. A.; Reinfelds, G.; Revzin, A. *Rev. Sci. Instrum.* **1973**, *44*, 1602–1609.

(59) Rad, J. A.; Albright, J. G.; Miller, D. G.; Zeidler, M. E. *J. Chem. Soc., Faraday Trans.* **1996**, *92*, 4187–4197.

(60) Yang, M. C.; Albright, J. G.; Rad, J. A.; Miller, D. G. *J. Solution Chem.* **1998**, *27*, 309–329.

(61) Miller, D. G.; Albright, J. G.; Mathew, R.; Lee, C. M.; Rad, J. A.; Eppstein, L. B. *J. Phys. Chem.* **1993**, *97*, 3885–3899.

(62) Miller, D. G.; Vitagliano, V. *J. Phys. Chem.* **1986**, *90*, 1706–1717.

(63) Miller, D. G. *J. Phys. Chem.* **1988**, *92*, 4222–4226.

(64) Mathew, R.; Paduano, L.; Albright, J. G.; Miller, D. G.; Rad, J. A. *J. Phys. Chem.* **1989**, *93*, 4370–4374.

(65) Mathew, R.; Albright, J. G.; Miller, D. G.; Rad, J. A. *J. Phys. Chem.* **1990**, *94*, 6875–6878.

(66) Creeth, J. M. *J. Am. Chem. Soc.* **1955**, *77*, 6428–6440.

(67) Creeth, J. M.; Gosting, L. J. *J. Phys. Chem.* **1958**, *62*, 58–65.

(68) Albright, J. G.; Miller, D. G. *J. Phys. Chem.* **1972**, *76*, 1853–1857.

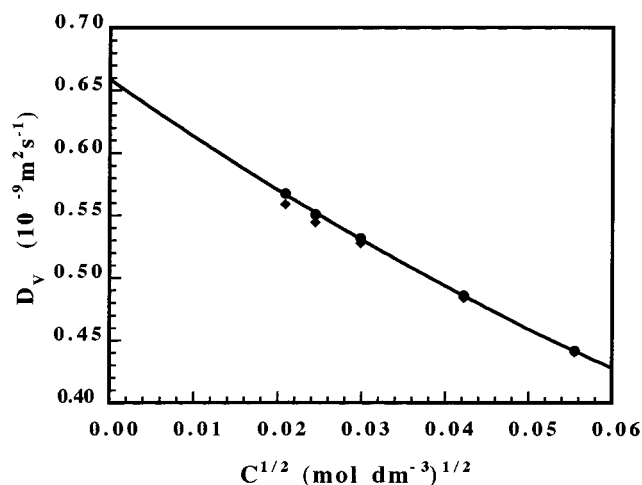


**Figure 1.** Diffusion coefficients of the binary system lysozyme chloride/water at pH 4.5 and 25 °C: ◆, experimental values, and ●, corrected values.

concentration. The limiting diffusion coefficients of  $2.03 \times 10^{-9}$  and  $9.37 \times 10^{-9} \text{ m}^2 \text{ s}^{-1}$  for the chloride and hydrogen ions, respectively, were obtained from the limiting ionic conductances.<sup>69</sup> The estimate of 6.7 for the charge of the protein is based on Nernst–Hartley (i.e., infinite dilution) theory and is described below in the Discussion section.

(2) The N–H equation is then used to calculate a diffusion coefficient for the binary system lysozyme  $\text{Cl}_{6.7}/\text{water}$  (the binary  $D_A$ ). We note that the value of 6.7 refers to the actual average charge of the protein, which differs from the stoichiometric value.

(3) The extended N–H equation for ternary systems<sup>2</sup> is now applied to the ternary system lysozyme chloride/HCl/water. Using the HCl concentration of  $3.16 \times 10^{-5} \text{ M}$  for pH 4.5, the four  $(D_{ij})_v$  values were calculated for each experiment. The value of  $D_A$  was calculated for each experiment from these  $(D_{ij})_v$  values, with the assumption that the refractive index increment  $R_1$  for the protein was much greater than  $R_2$  for the HCl ( $R_i \equiv [\partial n/\partial C_i]$ ), and the fact that  $\Delta C_2 = 0$ .

(4) For each concentration of lysozyme chloride, we computed a ratio of  $D_A$  calculated assuming ternary diffusion and the extended N–H equations to  $D_A$  calculated assuming binary diffusion and the binary N–H equation. This ratio was then used as a multiplicative factor to correct the measured binary diffusion coefficient. Figure 1 shows the measured and corrected values, along with the curve  $\gamma_0 + \gamma_1 C_1^{1/2} + \gamma_2 C_1$ , whose coefficients were determined from the corrected values by a least-squares fit.

Two experiments attempted at lower concentrations (0.09 and 0.15 mM) gave scattered results and are not included here. Self-buffering in these systems is at best marginal, and indeed it was difficult to adjust their pH, especially for the diluter top solutions.

An important diagnostic for free-diffusion experiments is a Rayleigh  $\Omega$  graph plotted vs  $f(j)$  for  $f(j)$  between 0 and 1.<sup>66,67,70</sup> In an ideal binary diffusion experiment, i.e., with a concentration-independent diffusion coefficient and a refractive index depending linearly on concentration, the values of  $\Omega_j$  (essentially the deviation of the  $j$ th fringe location from its position if the solution were “ideal”) should be zero for all values of  $f(j)$ . Thus,

**Table 2.** Ternary Experimental Data at 25 °C,  $[\text{NaCl}] = 0.25 \text{ M}$  (Series LNC2)

expt	LNC22	LNC23b	LNC23d	LNC24
$\bar{C}_1$ (mM)	0.6000	0.6000	0.6000	0.6000
$\bar{C}_2$ (M)	0.2500	0.2500	0.2500	0.2500
$\Delta C_1$ (mM)	0.0000	0.4000	0.4066	0.0000
$\Delta C_2$ (M)	0.1108	0.0000	0.0000	0.1108
pH bottom	4.51	4.51	4.50	4.50
pH top	4.50	4.50	4.50	4.48
$d$ ( $\text{g cm}^{-3}$ ) bottom	1.011 98 <sub>7</sub>	1.010 58 <sub>8</sub>	1.010 64 <sub>4</sub>	1.012 01 <sub>0</sub>
$d$ ( $\text{g cm}^{-3}$ ) top	1.007 50 <sub>7</sub>	1.008 93 <sub>0</sub>	1.008 96 <sub>4</sub>	1.007 55 <sub>2</sub>
$\Delta t$ (s)	7	34	31	10
$J$ (meas)	50.825	51.359	52.112	50.776
$J$ (calc)	50.800	51.311	52.159	50.800
$D_A$ (meas) ( $10^{-9} \text{ m}^2 \text{ s}^{-1}$ )	1.670	0.1294	0.1293	1.676
$D_A$ (calc) ( $10^{-9} \text{ m}^2 \text{ s}^{-1}$ )	1.738	0.1291	0.1291	1.738

nonzero  $\Omega$  values may indicate that either experiments are not truly binary, the diffusion coefficient depends significantly on concentration, or there is significant nonlinearity in the dependence of refractive index on concentration. Small values of  $\Omega$  strongly suggest that such potential problems are unimportant, and specifically that impurities are absent and aggregation is negligible.

Our  $\Omega$  values at lower concentrations were small but greater than the experimental uncertainty. Contributions to  $\Omega$  are expected both from the  $C^{1/2}$  dependence of binary diffusion coefficients at low concentrations<sup>48,71,72</sup> and from the increasingly ternary character of the system as  $C$  decreases, with HCl as the second solute. That the measured values of  $\Omega$  at the highest concentrations were not overly large and the remainder were quite small provides additional evidence that, except for water and chloride ions, the as-received protein was essentially pure. (We note that  $\Omega$  graphs from free-diffusion experiments performed with Gouy and Rayleigh interferometric optics have similar sensitivities to impurities.) Creeth<sup>73</sup> used the Rayleigh method to investigate the influence on  $\Omega$  of  $\sim 1.0 \text{ wt } \%$  solute impurity. He performed a series of experiments with sucrose impurity in urea, with urea impurity in sucrose, and with three proteins of uncertain purity, and found positive  $\Omega$  values significantly larger than could be attributed to instrumental uncertainty. Comparison of Creeth's  $\Omega$  values to ours supports the conclusion that any impurities other than water and chloride in our protein had essentially no effect on our interferometric diffusion measurements.

**Ternary Experiments at pH 4.5.** Ternary diffusion experiments were performed on the system lysozyme chloride/NaCl/water in the manner described elsewhere for nonprotein systems.<sup>59,60</sup> In all runs, there were  $\sim 50$  fringes in the Rayleigh fringe pattern. To obtain the four ternary diffusion coefficients, four experiments were performed at the same mean concentrations but with different values of  $\Delta C_i$  for the solutes. At each mean NaCl concentration of 0.25, 0.50, 0.65, and 0.90 M, there were two experiments with  $\Delta C_1 = 0$  and  $\Delta C_2 \neq 0$  and two with  $\Delta C_1 \neq 0$  and  $\Delta C_2 = 0$ . At 1.30 M NaCl, there were two experiments with  $\Delta C_1 = 0$  and  $\Delta C_2 \neq 0$  as before. However, for  $\Delta C_2 = 0$ , the protein concentration in the bottom solution required to obtain  $\sim 50$  fringes led to crystallization. Thus, as shown in Table 6, we made two runs with a reduced  $\Delta C_1$  and a small  $\Delta C_2$  [giving  $\alpha_1 = R_1 \Delta C_1 / (R_1 \Delta C_1 + R_2 \Delta C_2) = 0.8$  instead of 1.0] to achieve  $\sim 50$  fringes without crystallization.

Tables 2–6 show the data from five sets of experiments, where each set is at a different mean concentration of NaCl but

(69) Robinson, R. A.; Stokes, R. H. *Electrolyte Solutions*, 2nd ed.; Butterworths: London, 1970.

(70) Albright, J. G.; Sherrill, B. C. *J. Solution Chem.* **1979**, 8, 201–215.

(71) Albright, J. G.; Miller, D. G. *J. Phys. Chem.* **1975**, 79, 2061–2068.

(72) Albright, J. G.; Miller, D. G. *J. Phys. Chem.* **1980**, 84, 1400–1413.

(73) Creeth, J. M. *J. Phys. Chem.* **1958**, 62, 66–74.



**Table 3.** Ternary Experimental Data at 25 °C, [NaCl] = 0.50 M (Series LNC1)

expt	LNC11c	LNC12	LNC13	LNC14
$\bar{C}_1$ (mM)	0.6000	0.6000	0.6000	0.6000
$\bar{C}_2$ (M)	0.5000	0.5000	0.5000	0.5000
$\Delta C_1$ (mM)	0.4000	0.0000	0.4001	0.0000
$\Delta C_2$ (M)	0.0000	0.1136	0.0000	0.1136
pH bottom	4.50	4.51	4.51	4.50
pH top	4.50	4.51	4.50	4.48
$d$ (g cm <sup>-3</sup> ) bottom	1.02060 <sub>7</sub>	1.022 06 <sub>0</sub>	1.020 59 <sub>5</sub>	1.022 06 <sub>0</sub>
$d$ (g cm <sup>-3</sup> ) top	1.018 97 <sub>1</sub>	1.017 52 <sub>4</sub>	1.018 96 <sub>5</sub>	1.01752 <sub>9</sub>
$\Delta t$ (s)	62	6	56	8
$J$ (meas)	51.127	51.104	51.157	50.992
$J$ (calc)	51.138	51.054	51.145	51.043
$D_A$ (meas) (10 <sup>-9</sup> m <sup>2</sup> s <sup>-1</sup> )	0.1236	1.592	0.1238	1.676
$D_A$ (calc) (10 <sup>-9</sup> m <sup>2</sup> s <sup>-1</sup> )	0.1236	1.632	0.1236	1.632

**Table 4.** Ternary Experimental Data at 25 °C, [NaCl] = 0.65 M (Series LNC3)

expt	LNC31b	LNC32b	LNC33	LNC34
$\bar{C}_1$ (mM)	0.6000	0.6000	0.6000	0.6000
$\bar{C}_2$ (M)	0.6500	0.6500	0.6500	0.6500
$\Delta C_1$ (mM)	0.4000	0.0000	0.4001	0.0000
$\Delta C_2$ (M)	0.0000	0.1108	0.0000	0.1108
pH bottom	4.50	4.51	4.51	4.50
pH top	4.50	4.49	4.50	4.49
$d$ (g cm <sup>-3</sup> ) bottom	1.026 63 <sub>9</sub>	1.027 97 <sub>1</sub>	1.026 63 <sub>8</sub>	1.027 98 <sub>4</sub>
$d$ (g cm <sup>-3</sup> ) top	1.024 96 <sub>1</sub>	1.023 60 <sub>9</sub>	1.024 97 <sub>0</sub>	1.023 59 <sub>9</sub>
$\Delta t$ (s)	46	5	31	11
$J$ (meas)	51.999	49.234	51.990	49.223
$J$ (calc)	52.005	49.232	51.974	49.224
$D_A$ (meas) (10 <sup>-9</sup> m <sup>2</sup> s <sup>-1</sup> )	0.1209	1.580	0.1206	1.676
$D_A$ (calc) (10 <sup>-9</sup> m <sup>2</sup> s <sup>-1</sup> )	0.1208	1.616	0.1207	1.617

**Table 5.** Ternary Experimental Data at 25 °C, [NaCl] = 0.90 M (Series LNC4)

expt	LNC41	LNC42	LNC43	LNC44
$\bar{C}_1$ (mM)	0.6000	0.6000	0.6000	0.6000
$\bar{C}_2$ (M)	0.8999	0.9000	0.9000	0.8999
$\Delta C_1$ (mM)	0.4000	0.0000	0.4000	0.0000
$\Delta C_2$ (M)	0.0000	0.1108	0.0000	0.1108
pH bottom	4.51	4.51	4.50	4.50
pH top	4.50	4.50	4.47	4.50
$d$ (g cm <sup>-3</sup> ) bottom	1.036 40 <sub>8</sub>	1.037 75 <sub>1</sub>	1.036 40 <sub>8</sub>	1.037 75 <sub>2</sub>
$d$ (g cm <sup>-3</sup> ) top	1.034 76 <sub>5</sub>	1.033 42 <sub>2</sub>	1.034 76 <sub>3</sub>	1.033 42 <sub>0</sub>
$\Delta t$ (s)	25	11	29	8
$J$ (meas)	51.045	48.471	51.094	48.391
$J$ (calc)	51.069	48.435	51.070	48.426
$D_A$ (meas) (10 <sup>-9</sup> m <sup>2</sup> s <sup>-1</sup> )	0.1174	1.574	0.1175	1.577
$D_A$ (calc) (10 <sup>-9</sup> m <sup>2</sup> s <sup>-1</sup> )	0.1174	1.611	0.1174	1.611

all sets have the same mean concentration of 0.60 mM lysozyme. Included are mean concentrations of both solutes,  $\Delta C_i$  values across the starting boundary, densities and pH values of the top and bottom solutions, and  $\Delta t$  determined as described above for the binary case. The experimental values of  $J$  are listed for each experiment. Calculated values of  $J$  for each set of initial  $\Delta C_i$  values are included in Tables 2–6 for comparison and usually agree very well with experiment. The coefficients  $R_1$  and  $R_2$  needed to calculate  $J = R_1\Delta C_1 + R_2\Delta C_2$  were obtained by the method of least squares from the experimental data for each set of mean concentrations and are shown in Table 7. Note that they depend very little on mean concentration.

Rayleigh  $D_A$  values for each experiment are obtained as follows. The measured  $D_j$  (after applying the appropriate  $\Delta t$  offset) for a given symmetrical fringe pair  $j$  is averaged over all the scans of the experiment. The square-root of this average,  $\sqrt{D_j}$ , and its corresponding  $z_j^2$  (see above) are calculated. These quantities for all the fringe pairs are then extrapolated linearly

**Table 6.** Ternary Experimental Data at 25 °C, [NaCl] = 1.30 M (Series LNC5)

expt	LNC51	LNC52	LNC53	LNC54
$\bar{C}_1$ (mM)	0.5999	0.5999	0.5999	0.5999
$\bar{C}_2$ (M)	1.2999	1.2999	1.2999	1.2999
$\Delta C_1$ (mM)	0.3200	0.0000	0.3200	0.0000
$\Delta C_2$ (M)	0.0222	0.1108	0.0222	0.1107
pH bottom	4.52	4.51	4.50	4.49
pH top	4.50	4.50	4.50	4.50
$d$ (g cm <sup>-3</sup> ) bottom	1.052 16 <sub>3</sub>	1.053 21 <sub>4</sub>	1.052 15 <sub>8</sub>	1.053 20 <sub>6</sub>
$d$ (g cm <sup>-3</sup> ) top	1.049 97 <sub>0</sub>	1.048 95 <sub>7</sub>	1.049 97 <sub>2</sub>	1.048 95 <sub>3</sub>
$\Delta t$ (s)	19	24	8	24
$J$ (meas)	50.149	47.288	50.167	47.197
$J$ (calc)	50.158	47.259	50.158	47.226
$D_A$ (meas) (10 <sup>-9</sup> m <sup>2</sup> s <sup>-1</sup> )	0.1510	1.579	0.1507	1.582
$D_A$ (calc) (10 <sup>-9</sup> m <sup>2</sup> s <sup>-1</sup> )	0.1515	1.617	0.1515	1.617
$D_{DLS}$ bottom (10 <sup>-9</sup> m <sup>2</sup> s <sup>-1</sup> )	0.105 <sub>3</sub>	0.108 <sub>6</sub>	0.105 <sub>1</sub>	0.108 <sub>8</sub>
$D_{DLS}$ top (10 <sup>-9</sup> m <sup>2</sup> s <sup>-1</sup> )	0.114 <sub>3</sub>	0.110 <sub>5</sub>	0.114 <sub>8</sub>	0.111 <sub>9</sub>

to  $z_j^2 = 0$  (i.e., to the center of the Rayleigh pattern) to get the square-root of  $D_A$  and thus  $D_A$  itself.<sup>74</sup> For comparison, a calculated value of  $D_A$  for each experiment is included in Tables 2–6. Each calculated  $D_A$  is obtained from the values of  $\Delta C_i$ ,  $R_i$ , and the four  $(D_{ij})_v$  for each set of experiments at the same mean concentrations.<sup>46</sup> The two  $D_A$  values agree well for experiments starting with only lysozyme gradients but show small errors for those starting with only NaCl gradients, probably because of the difficulty in extrapolating the  $D_j$  curves in these cases.

Figure 2 presents the concentrations at which the ternary experiments were performed, as well as the solubility curve for tetragonal lysozyme at pH 4.5 as a function of NaCl concentration.<sup>75</sup> It also shows the difference in the concentration of protein (vertical range bars) or NaCl (horizontal range bars) between the top and bottom solutions used in the experiments. Figure 3 shows (with different scales) the four diffusion coefficients for the system lysozyme chloride/NaCl/H<sub>2</sub>O versus NaCl molarity. The mean concentration of lysozyme chloride is fixed at 0.60 mM, whereas the mean concentration of NaCl varies from 0.25 to 1.30 M. As can be seen from Figures 2 and 3, at the mean NaCl concentration of 0.90 M, the mean composition corresponds to supersaturated conditions, as do the bottom solutions in all four experiments at that mean NaCl concentration, and the top solutions in experiments LNC42 and LNC44. For 1.30 M, all top and bottom solutions are supersaturated.

**Partial Molar Volumes.** Values of  $\bar{V}_1$  and  $\bar{V}_0$  in Table 1 were calculated by letting  $\Delta d/\Delta C$  approximate the density derivative [note that  $\Delta d = d(\text{bottom}) - d(\text{top})$ ] and applying eqs A-7 ( $q = 1$ ) and 5 in Dunlop and Gosting.<sup>76</sup>

Values of  $\bar{d}$  and  $H_i = (\partial d/\partial C_i)_{T,P,C_j,j \neq i}$  in Table 7 were calculated using densities of all eight solutions in each experimental set. Densities were assumed to be linear in solute concentrations, and values of  $\bar{d}$  and the  $H_i$  for the following equation were obtained by the method of least squares:

$$d = \bar{d} + H_1(C_1 - \bar{C}_1) + H_2(C_2 - \bar{C}_2) \quad (3)$$

Here  $\bar{C}_1$  and  $\bar{C}_2$  are the averages of the mean concentrations for all four experiments in a series. The  $\bar{V}_1$ ,  $\bar{V}_2$ , and  $\bar{V}_0$  values in Table 7 were calculated using eqs A-7 ( $q = 2$ ) and 5 in ref 76.

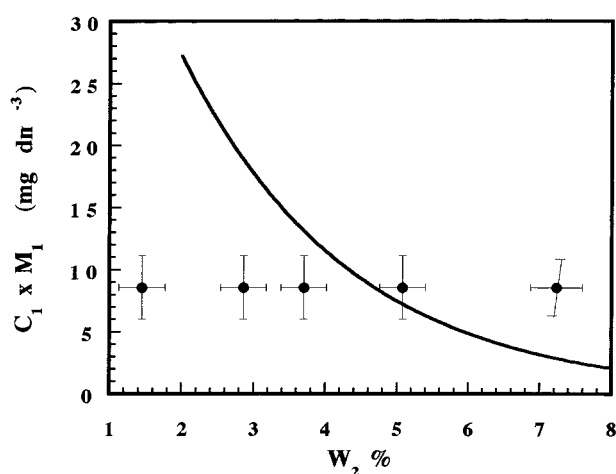
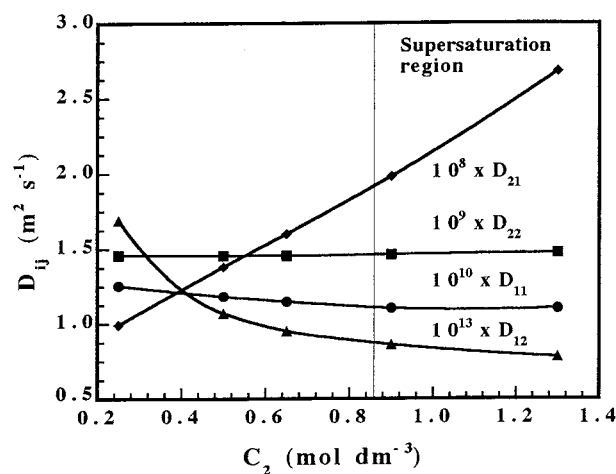
**Dynamic Light-Scattering Results.** Measured values of  $D_{DLS}$  are listed in Table 6 for each of the eight solutions used in the

(74) Miller, D. G. *J. Solution Chem.* **1981**, *10*, 831–846.(75) Howard, S. B.; Twigg, P. J.; Baird, J. K.; Meehan, E. J. *J. Cryst. Growth* **1988**, *90*, 94–104.(76) Dunlop, P. J.; Gosting, L. J. *J. Phys. Chem.* **1959**, *63*, 86–93.



**Table 7.** Derived Ternary Diffusion Data at 25 °C

series	LNC2	LNC1	LNC3	LNC4	LNC5
$\bar{C}_1$ (mM)	0.6000	0.6000	0.6000	0.6000	0.5999
$\bar{C}_2$ (M)	0.2500	0.5000	0.6500	0.9000	1.2999
$\bar{d}$ (g cm <sup>-3</sup> )	1.009 75 <sub>1</sub>	1.019 78 <sub>9</sub>	1.025 79 <sub>7</sub>	1.035 58 <sub>8</sub>	1.051 07 <sub>4</sub>
$H_1$ (10 <sup>3</sup> g mol <sup>-1</sup> )	4.124	4.080	4.180	4.110	4.182
$H_2$ (10 <sup>3</sup> g mol <sup>-1</sup> )	0.040 42	0.039 90	0.039 45	0.039 07	0.038 41
$\bar{V}_1$ (cm <sup>3</sup> mol <sup>-1</sup> )	10 215	10 254	10 151	10 218	10 139
$\bar{V}_2$ (cm <sup>3</sup> mol <sup>-1</sup> )	18.094	18.592	18.988	19.383	20.061
$\bar{V}_0$ (cm <sup>3</sup> mol <sup>-1</sup> )	18.067	18.063	18.059	18.053	18.041
$R_1$ (10 <sup>2</sup> dm <sup>3</sup> mol <sup>-1</sup> )	1283	1278	1300	1277	1272
$R_2$ (10 <sup>2</sup> dm <sup>3</sup> mol <sup>-1</sup> )	4.585	4.494	4.443	4.371	4.264
$S_A/I_A$	2.669	2.634	2.660	2.670	2.849
$\lambda_1$ (10 <sup>-9</sup> m <sup>2</sup> s <sup>-1</sup> )	0.1241	0.1170	0.1136	0.1089	0.1015
$\lambda_2$ (10 <sup>-9</sup> m <sup>2</sup> s <sup>-1</sup> )	1.460	1.456	1.456	1.463	1.476
$(D_{11})_v$ (10 <sup>-9</sup> m <sup>2</sup> s <sup>-1</sup> )	0.1254 ± 0.0001	0.1182 ± 0.0001	0.1147 ± 0.0001	0.1102 ± 0.0001	0.1031 ± 0.0001
$(D_{12})_v$ (10 <sup>-9</sup> m <sup>2</sup> s <sup>-1</sup> )	0.000 169 ± 0.000 002	0.000 107 ± 0.000 002	0.000 095 ± 0.000 001	0.000 086 ± 0.000 002	0.000 078 ± 0.000 001
$(D_{21})_v$ (10 <sup>-9</sup> m <sup>2</sup> s <sup>-1</sup> )	9.9 ± 0.2	13.8 ± 0.2	16.0 ± 0.1	19.8 ± 0.2	26.8 ± 0.2
$(D_{22})_v$ (10 <sup>-9</sup> m <sup>2</sup> s <sup>-1</sup> )	1.459 ± 0.001	1.455 ± 0.001	1.455 ± 0.001	1.461 ± 0.001	1.475 ± 0.001

**Figure 2.** Ternary points in the phase diagram at pH 4.5 and 25 °C: ● denotes average composition. The horizontal bars give  $\Delta C_2$  in weight percent NaCl for experiments with  $\Delta C_1 = 0$ , and the vertical bars give  $\Delta C_1 M_1$  (in g dm<sup>-3</sup>) for experiments with  $\Delta C_2 = 0$ . The solid curve represents the solubility data.<sup>75</sup>**Figure 3.** Diffusion coefficients of the ternary system lysozyme chloride/NaCl/water at pH 4.5 and 25 °C.

LNC5 ternary series at 1.30 M NaCl. The precision is  $\pm 1\%$ . We note that the lysozyme concentration in the top and bottom solutions in experiments LNC52 and LNC54 is the same as the mean lysozyme concentration (0.60 mM) in all of the free-diffusion experiments. If we average the  $D_{DLS}$  values from the top and bottom solutions in LNC52 and LNC54, we obtain an

approximation to  $D_{DLS}$  at the mean NaCl concentration in those experiments, thus allowing direct comparison to the interferometric  $(D_{11})_v$  at 1.30 M NaCl (Table 7). These average values of  $D_{DLS}$  are approximately 6% higher than  $(D_{11})_v$  and approximately 8% higher than the smallest eigenvalue ( $0.1016 \pm 0.0002 \times 10^{-9} \text{ m}^2 \text{ s}^{-1}$ ) of the matrix of diffusion coefficients, the  $D_{DLS}$  predicted by Leaist's theory.<sup>27</sup> These discrepancies may be due to the dependence of  $D_{DLS}$  on scattering angle or other instrumental parameters not selectable in our light-scattering apparatus.

## Discussion

**Aqueous Binary Lysozyme Chloride<sub>6.7</sub> Solutions.** Since the binary system lysozyme Cl<sub>6.7</sub>/water is an electrolyte solution, the dependence of  $D_v$  on concentration  $C$  is usefully described by a polynomial in  $C^{1/2}$ , as predicted by the Debye–Hückel theory. A least-squares quadratic in  $C^{1/2}$ ,

$$D_v = 0.6607(1 - 7.21C^{1/2} + 22.2C) \quad (4)$$

represents the corrected  $D_A$  (see above) in Table 1 very well, where  $C$  is in molar units and  $D_v$  is  $10^{-9} \text{ m}^2 \text{ s}^{-1}$ .

For binary electrolyte solutions, the N–H equation relates  $D_v$  at infinite dilution to the intrinsic mobilities and charges of the ions:

$$D^0 = \frac{(z_+ - z_-)D_+^0 D_-^0}{D_+^0 z_+ - D_-^0 z_-} \quad (5)$$

Here,  $D_+^0$  and  $D_-^0$  are the infinite dilution tracer diffusion coefficients for the lysozyme ( $0.12 \times 10^{-9} \text{ m}^2 \text{ s}^{-1}$ ) and chloride ( $9.37 \times 10^{-9} \text{ m}^2 \text{ s}^{-1}$ ) ions, respectively (see above), and  $z_+$  and  $z_-$  are the charges on the ions. By applying this formula to our system, we can estimate an effective charge on the protein.

As noted in the Results section, the measured binary diffusion coefficients were corrected for added HCl to obtain the true ones using the binary and ternary N–H equations. The N–H equations depend on the unknown charge of the lysozyme. Consequently, several iterations, starting from an initial estimate, were necessary to find the final value of  $z_+$ . The value obtained by this procedure, 6.7, is smaller than the corresponding  $z_+ = 11$  from the titration curve.<sup>77</sup> However, the effective charge of a polyelectrolyte is almost always smaller than the stoichiometric

(77) Tanford, C.; Wagner, M. L. *J. Am. Chem. Soc.* **1954**, *76*, 3331–3336.

value because of the presence of counterions in the motion sphere of the polyvalent ion. In our case, approximately four chloride ions move in the hydrodynamic motion sphere of each lysozyme molecule.

For a binary electrolyte solution at low concentration, the concentration dependence of  $D_v$  is given approximately by the following equation:

$$D_v = D^0(1 + d \ln y/d \ln C) \quad (6)$$

This equation was applied to aqueous lysozyme chloride solutions, assuming that the logarithmic derivative of the activity coefficient  $y$  can be calculated from the simple Debye–Hückel equation at 25 °C:

$$\frac{d \ln y}{d \ln C} = -0.587 z_+ [(z_+^2 + z_-)C/2]^{1/2} \quad (7)$$

where  $z_-$  (not shown) is  $-1$ . Using  $z_+ = 4$  yields the limiting slope of  $D_v$  versus  $C^{1/2}$  presented in eq 4, which differs from the value of 6.7 obtained by extrapolation. Of course, the Debye–Hückel equation cannot be appropriate for large molecular ions with many distributed charge sites. However, the result is interesting and ultimately may give an approximate method to estimate the activity coefficients of lysozyme chloride in aqueous binary solutions at 25 °C.

**Ternary Lysozyme Chloride/NaCl/H<sub>2</sub>O Solutions.** We see from Table 7 and Figure 3 that the cross-term diffusion coefficient  $(D_{21})_v$  for the flux of NaCl caused by a gradient of lysozyme chloride increases sharply as the NaCl concentration increases. In fact, at 1.30 M NaCl, it becomes more than 18 times as large as the NaCl main-term diffusion coefficient  $(D_{22})_v$ . At this NaCl concentration, the ratio  $(D_{21})_v/(D_{11})_v$  is 259, so that with a gradient of lysozyme alone, diffusion of each lysozyme molecule would be accompanied by equimolar fluxes of 259 Na<sup>+</sup> and Cl<sup>−</sup> ions. This indicates that, as lysozyme diffuses to the surface of a crystal in the crystallization process, there will be a buildup of NaCl. This in turn would lower the lysozyme solubility at the crystal surface (cf. Figure 2). Similarly, the ratio  $(D_{22})_v/(D_{12})_v$  is approximately 18 900, indicating that a flux of 18 900 NaCl ion pairs is required in order to transport each lysozyme molecule in a system in which the protein concentration is uniform. Therefore, a gradient of NaCl near the crystal surface will not significantly impede diffusion of lysozyme toward the surface. We note that the availability of  $(D_{11})_v$  and  $(D_{21})_v$  allows one to use a phenomenologically faithful description of multicomponent transport to compute the flux of NaCl driven by a lysozyme gradient (e.g., as in salt rejection at a growing crystal), without the approximations inherent in the approaches of Lin et al.<sup>8</sup> and Grant and Saville.<sup>9</sup>

For lysozyme in undersaturated or slightly supersaturated aqueous sodium acetate buffer with 4 wt % NaCl at pH 4.0 and 25 °C, pseudobinary diffusion coefficients varying with solution age (up to 160 h) have been reported.<sup>78</sup> In one case, the diffusion coefficient decreased by 40% after 25 h.

We observed no time dependence during our experiments, which were never longer than 4 h and were always completed within 10 h of the start of solution preparation. In addition, an important and sensitive diagnostic for these experiments is obtained from values of  $D_{ave}$  calculated for each scan on the basis of the same average of  $D_j$  values used to calculate binary diffusion coefficients as described above. These averages have

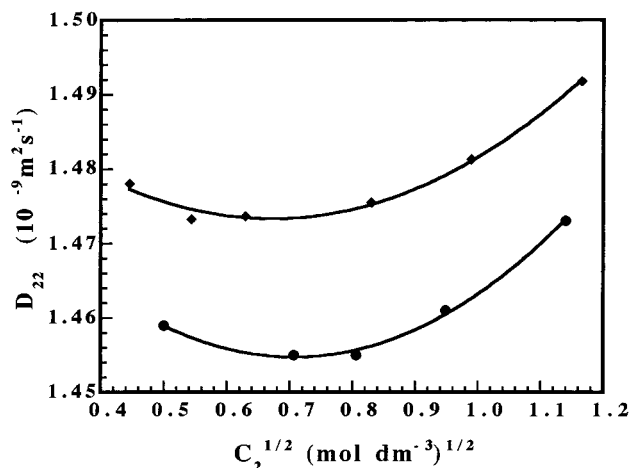


**Figure 4.** Diffusion coefficients: ♦ denotes  $D_v$  for the binary system NaCl/water (Rard and Miller<sup>79</sup>), and ● denotes  $(D_{22})_v$  from Table 7.

no physical interpretation for multicomponent systems, but values obtained from each of 50 scans during an experiment should lie on a straight line when plotted versus  $1/t$ . The straightness of these plots, used to get  $\Delta t$  for a ternary experiment, provides a good diagnostic for the quality of the experiment, since protein degradation, aggregation, or other phenomena responsible for time-dependent solution properties contribute to curvature. However, in our experiments, these diagnostic lines were so straight that the  $\Delta t$ -corrected  $D_{ave}$  values were constant to within a few tenths of a percent during the 4-h experimental duration. Duplicate experiments were consistent within 1 part per thousand for the main-term diffusion coefficients, again indicating that any temporal changes in solution properties differed by less than 0.2% between experiments.

**Characteristics of the  $(D_{ij})_v$ .** The large variation of  $(D_{21})_v$  with NaCl concentration (cf. Figure 3) may be primarily due to an excluded volume effect. Increasing the lysozyme chloride concentration at constant NaCl molarity will increase the “effective” concentration of NaCl in the solution between the lysozyme ions. Given a uniform bulk concentration of NaCl in a gradient of lysozyme chloride, there will be an effective concentration gradient of NaCl that is directly proportional to the lysozyme chloride gradient. This in turn will drive a flux of NaCl from higher to lower lysozyme chloride concentration regions, which will be reflected in a large positive  $(D_{21})_v$  coefficient in the flux equations (eq 1 for ternary cases). On the other hand,  $(D_{12})_v$  is small and decreases as the salt concentration increases. Figure 4 shows that the ternary main-term  $(D_{22})_v$  lies within 1% or 2% of the binary solution  $D_v$  over the entire composition range, as expected. The slightly lower ternary value can be attributed to the large protein molecules obstructing the flux of the small ions. Finally, it is difficult to say much about  $(D_{11})_v$  compared to its binary value because the lysozyme chloride, while not quite present in trace amounts, is still at a small concentration compared to that of its NaCl supporting electrolyte. The coefficient  $(D_{11})_v$  is the one that pseudobinary diffusion coefficients ought to approximate when measured at the same pH and NaCl concentrations.

Our results are very reproducible and thus very precise. However, we are aware that one should be particularly cautious about claims of accuracy when one of the solutes is a protein. Without specifying a level of accuracy, we believe the results to be accurate within a few multiples of the precision indicated in the tables.

**Convergence Diagnostics.** The convergence of TFIT, our nonlinear least-squares program, depends on the eigenvalues

(78) Kim, Y.-C.; Myerson, A. S. *J. Cryst. Growth* **1994**, *143*, 79–85.

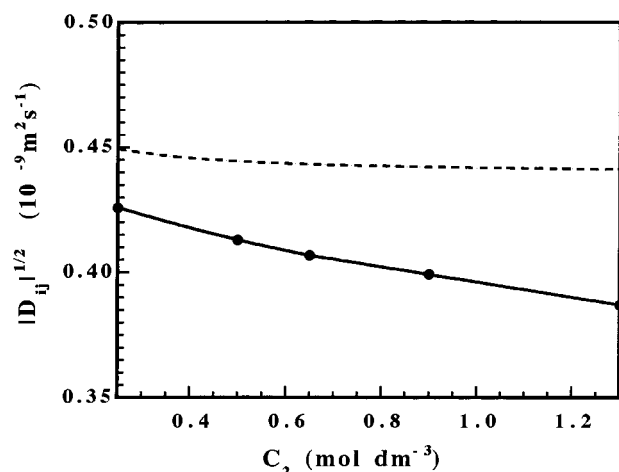


**Figure 5.** Nernst-Hartley values of  $|D_{ij}|$  (---). Experimental values of  $|D_{ij}|$  (—).

$\lambda_1$  and  $\lambda_2$  being distinct and  $S_A^{46,47}$  (or  $S_A/I_A$ ) being relatively large.<sup>61</sup> Table 7 shows that these conditions are satisfied. That  $\lambda_1$  and  $\lambda_2$  are close to  $(D_{11})_v$  and  $(D_{22})_v$ , respectively, is a consequence of  $D_{12}$  being very small. The values of  $S_A$ ,  $I_A$ , and  $S_A/I_A$  fall in the ranges 634–694, 240–249, and 2.63–2.85, respectively.

**Behavior of  $|D_{ij}|$ .** Figure 5 shows the NaCl dependence of the determinant of the diffusion coefficient matrix,  $|D_{ij}| = (D_{11})_v(D_{22})_v - (D_{12})_v(D_{21})_v$ , computed from measured diffusion coefficients as well as from the N-H theory. The N-H  $|D_{ij}|$  decreases slightly with NaCl molarity. The measured  $|D_{ij}|$  decreases more but still remains large at the supersaturated mean concentrations 0.90 and 1.30 M. The cross-term product  $(D_{12})_v(D_{21})_v$  is only 1–2% of  $(D_{11})_v(D_{22})_v$ , and the decrease in  $|D_{ij}|$  is primarily due to the decrease in  $(D_{11})_v$ .

Since  $|D_{ij}|$  must vanish on a spinodal curve in the isobaric, isothermal ternary phase plane,<sup>12,80–83</sup> a (1 atm, 25 °C) spinodal point for 0.60 mM lysozyme chloride, if one exists, must occur at a NaCl concentration greater than 1.30 M. This issue is significant because Muschol and Rosenberger<sup>29</sup> report spinodal curves in the quaternary lysozyme chloride/NaCl/0.1 M acetate (NaAc/HAc buffer)/H<sub>2</sub>O system at pH 4.5. Their lysozyme chloride concentrations (40–400 mg/mL) were much higher than our 8.5 mg/mL, but their NaCl concentrations (3–7% w/v) were within our range (1.5–7% w/v). Whether  $|D_{ij}|$  falls slowly or precipitously as the spinodal is approached at either fixed NaCl or lysozyme chloride concentration is an open question,<sup>84</sup> closely related to the issue of how each  $(D_{ij})_v$  varies.

(79) Rard, J. A.; Miller, D. G. *J. Solution Chem.* **1979**, *8*, 701–716.

(80) Sundelöf, L.-O. *Ark. Kemi.* **1963**, *20*, 369–384.

(81) Lo, P. Y.; Myerson, A. S. *AIChE J.* **1989**, *35*, 676–677.

(82) Kirkaldy, J. S.; Purdy, G. R. *Can. J. Phys.* **1969**, *47*, 865–871.

(83) Ziebold, T. O.; Ogilvie, R. E. *Trans. Metall. Soc. AIME* **1967**, *239*, 942–953.

(84) Few data indicate how  $|D_{ij}|$  will vary along a “concentration trajectory” in the ternary phase plane as a spinodal is approached. Clearly, there are contours of constant  $|D_{ij}|$  in that plane, with the curve  $|D_{ij}| = 0$  corresponding to the spinodal. In the system chloroform/acetic acid/water at 25 °C, Vitagliano et al.<sup>12</sup> approached the known spinodal curve along a trajectory on which the water/chloroform ratio was approximately constant and found that  $|D_{ij}|$  decreased to zero nearly linearly over a wide range of composition. In that case, the angle between the concentration trajectory and the tangent to the spinodal was approximately 80° in the triangular three-component, isothermal isobaric phase diagram. On the other hand, for the system glycine/L-valine/water at 25 °C, Lo and Myerson<sup>81</sup> observed a precipitous drop in  $|D_{ij}|$  with increasing glycine molarity at 0.05 M L-valine concentration, and used that drop-off to estimate the location of the spinodal point for 0.05 M L-valine. Since the spinodal curve is unknown for that system, the angle between it and the concentration trajectory cannot be estimated.

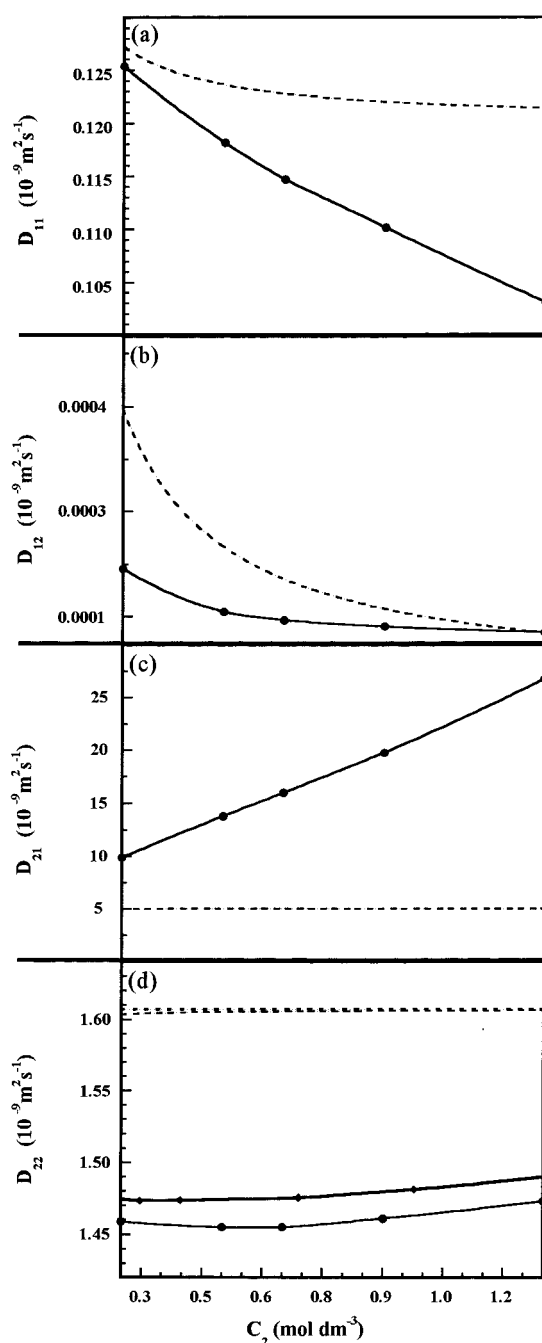


**Figure 6.** Comparison of experimental diffusion coefficients with Nernst-Hartley estimates. (a–d) ● denotes ternary  $(D_{ij})_v$ ; ternary Nernst-Hartley estimates (---). (d) ♦ denotes binary  $D_v$  for NaCl; binary Nernst-Hartley estimates (---).

These questions have important consequences for the kinetics of both protein crystal growth and liquid–liquid phase separation and will be addressed in our future measurements of  $(D_{ij})_v$  at higher lysozyme chloride concentrations than reported here.

**Partial Molar Volumes.** The partial molar volumes of lysozyme chloride from both the binary and ternary measurements were all about 10 200 mL mol<sup>−1</sup>. This corresponds to a density of the protein in solution of ~1.4 g/mL compared to the ~1.3 g/mL crystal value.

The  $\bar{V}_0$  and  $\bar{V}_2$  from the ternary experiments are similar to NaCl solution binary values at matching NaCl concentrations. However, on the average, ternary  $\bar{V}_2$  values are slightly higher. Because  $\bar{V}_2$  slowly increases as NaCl molarity increases, the



higher  $\bar{V}_2$  values are consistent with the higher effective NaCl concentrations between protein molecules.

**N-H Does Not Predict  $(D_{ij})_v$  in Concentrated Solutions.** Figure 6 shows comparisons of the measured  $(D_{ij})_v$  and the corresponding N-H estimates.<sup>2</sup> The N-H  $(D_{11})_v$  is higher but close to the measured  $(D_{11})_v$  at low concentrations but diverges with increasing NaCl concentration, being about 15% higher at the highest concentration. The N-H  $(D_{12})_v$  is more than twice the measured value at the lowest concentration, but in contrast to  $(D_{11})_v$ , the gap decreases at higher concentrations. Whether the gap between experimental values of  $(D_{12})_v$  and N-H theory will narrow as the NaCl concentration decreases will depend on the magnitude of activity coefficient effects (not accounted for by the theory) at  $C_1 = 0.60$  mM. For  $(D_{21})_v$ , the N-H value is essentially constant, being too low by a factor of 2 at low concentration and by a factor of 5 at high concentration. The N-H  $(D_{22})_v$  and  $D_v$  are uniformly about 10% higher than the measured values and are closer together than the measured  $(D_{22})_v$  and  $D_v$ . The N-H equations are helpful for interpretation and estimation in dilute solutions, as shown by Leaist's work.<sup>22-25</sup> However, in more concentrated solutions relevant to protein crystallization (including those near and above saturation in the present work), they clearly provide poor and even misleading estimates.

## Conclusion

We have presented the first complete set of multicomponent diffusion coefficients for a ternary system involving a protein at concentrations high enough to be relevant to crystallization studies. These very reproducible, and thus very precise, measurements make possible a more rigorous treatment than in previous work<sup>8</sup> of the effects of coupled salt and protein transport in the crystallization of the model protein lysozyme from aqueous NaCl solutions. They also point the way to more extensive measurements (e.g., at other protein concentrations, temperatures, and pH values) for this widely studied system as well as other protein systems.

**Acknowledgment.** The authors thank Pamela Bowman for her considerable help in performing a literature search for this work. The support of the NASA Biotechnology Program through Grant NAG8-1356 is gratefully acknowledged. A small portion of the work of D.G.M. was performed under the auspices of the U.S. Department of Energy, Office of Basic Energy Sciences, at Lawrence Livermore National Laboratory under Contract No. W-7405-ENG-48.

JA9834834